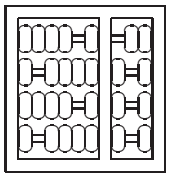

INSTITUTO DE COMPUTAÇÃO
UNIVERSIDADE ESTADUAL DE CAMPINAS

Wavelet-based Feature Extraction for Fingerprint Image Retrieval

Javier A. Montoya Zegarra *Neucimar J. Leite*
Ricardo da S. Torres

Technical Report - IC-06-012 - Relatório Técnico

September - 2006 - Setembro

Wavelet-based Feature Extraction for Fingerprint Image Retrieval

Javier A. Montoya Zegarra* Neucimar J. Leite Ricardo da S. Torres

Abstract

This paper presents a novel approach to fingerprint retrieval for personal identification by joining three image retrieval tasks, namely, feature extraction, similarity measurement, and feature indexing, into a wavelet-based fingerprint retrieval system.

We propose the use of different types of Wavelets for representing and describing the textural information present in fingerprint images. For that purposes, the feature vectors used to characterize the fingerprints are obtained by computing the mean and the standard deviation of the decomposed images in the Wavelet domain. These feature vectors are used to retrieve the most similar fingerprints given a query image, while their indexation is used to reduce the search spaces of image candidates. The different types of Wavelets used in our study include: Gabor Wavelets (GWs), Tree-Structured Wavelet Decomposition using both Orthogonal Filter Banks (TOWT) and Bi-orthogonal Filter Banks (TBOWT), as well as the Steerable Wavelets.

To evaluate the retrieval accuracy of the proposed approach, a total number of eight different data sets were used. Experiments also evaluated different combinations of Wavelets with six similarity measures. The results show that the Gabor Wavelets combined with the Square Chord similarity measure achieves the best retrieval effectiveness.

1 Introduction

Fingerprints are considered nowadays one of the most reliable biometric characteristic for human identification among other physical and behavioral characteristics, such as face [2], iris [3], voice [12], and gait [13]. Several fingerprint recognition applications in civilian, commercial and forensic systems are usually based on two basic fingerprint properties: [26] (1) persistence: basic fingerprint characteristics do not change with time and (2) individuality: each person has a unique fingerprint.

Automatic fingerprint recognition often involves four important steps [28, 29]: (1) acquisition, (2) classification, (3) identification, and (4) verification. Fingerprint acquisition is

*Research supported in part by CNPq — Conselho Nacional de Desenvolvimento Científico e Tecnológico, under grant #134990/2005-6

refered to the capture and representation of fingerprints. Fingerprint classification consists in assigning a fingerprint to a pre-defined class, whereas fingerprint identification is referred to the retrieval of fingerprints that correspond to a given fingerprint query image (one-to-many comparisons). Fingerprint verification is used to determine whether two fingerprint images are the same or not (one-to-one comparisons). Note that, considering the large size of fingerprint databases and the computational cost of fingerprint verification algorithms, it is necessary to reduce the number of one-to-many comparisons during fingerprint identification, seeking both accuracy and retrieval speed.

In this context, we propose an original approach to guide the search and the retrieval in fingerprint image databases. Our approach uses feature extraction and indexing methods based on texture information found in fingerprint images. For that purpose, we exploit the capability of the Wavelet transform to integrate both multiresolution and space-frequency properties in a natural manner [40]. By using the Wavelet decomposition property, the fingerprint images are decomposed into different spatial/frequency sub-images and some statistical analysis is performed to generate feature vectors. The extracted texture feature vectors are used to compute the similarity among images and, then to retrieve the most similar ones given a fingerprint query image.

In our approach, the texture features are extracted by different types of the Wavelet Transform, which include: Gabor Wavelet transform [23, 19] and Tree-Structured Wavelet Transform (TSWT) using both Orthogonal- and Bi-orthogonal Filterbanks [24, 20, 22, 21]. In the Gabor Wavelet transform, different scales and orientations are used to capture relevant texture information. In the case of the TSWT, the image texture content is captured on the low frequency subband, while the high frequency subbands are used to capture the image variations in different directions.

Similarity measures play an important role in the system's retrieval accuracy. Therefore, we have also evaluated several different similarity measures (Bray Curtis, Canberra, Euclidean, Manhattan, Square Chord and Square Chi-Squared distances) to be used for calculating the distances between the wavelet-based feature vectors.

Considering that the query processing time should only depend on the number of images that are similar to the fingerprint image query and not on the total number of fingerprints in the database, we employ the dynamic Metric Access Method (MAM) known as Slim-tree [38] for feature indexing purposes.

The main contributions of this work are summarized below:

1. A description of a texture-based retrieval system for fingerprint identification that can tolerate distorted fingerprint images and can be adapted according the user requirements.
2. A detailed comparison of the retrieval effectiveness achieved by different types of Wavelet-based multi-scale texture feature extraction mechanisms.

3. A comparative study of different similarity measures.

The remainder of this paper is organized as follows. Next section summarizes some related concepts, while section 3 reviews some approaches related to our work. Section 4 presents the architecture of our system. The various features extracting algorithms are described in section 6. Different similarity metrics and the feature indexing method are described in section 7. The experimental setup and the results of our tests are discussed in section 8. Finally, our conclusions and future work are described in section 9.

2 Background

In this section, we formalize the main terms related along this paper.

2.1 Image Descriptors

Definition 1. An **image descriptor** D is defined as a pair (ϵ_D, δ_D), where $\epsilon_D : I \rightarrow \mathbb{R}^n$ is a function that extract a feature vector $\vec{v_I}$ from a given image I, and $\delta_D : \mathbb{R}^n \text{x} \mathbb{R}^n \rightarrow \mathbb{R}^n$ denotes the distance function used to computed similarity between two images considering their feature vectors. The smaller the distance is, the more similar the images are.

Definition 2. A **feature vector** $\vec{v_I}$ of an image I is a point in $\mathbb{R}^n$ space, such that: $\vec{v_I} = (v_1, v_2, \ldots, v_n)$ and where n denotes the dimension of the vector.

2.2 Metric Spaces

Definition 3. A **metric distance** function $d()$ is a function that has the following properties:

(i) Symmetry: $d(O_1, O_2) = d(O_2, O_1)$

(ii) Positiveness: $0 < d(O_1, O_2) < \infty, \quad O_1 \neq O_2$ and $d(O_1, O_2) = 0$

(iii) Triangle inequality: $d(O_1, O_3) \leq d(O_1, O_2) + d(O_2, O_3)$

where O denotes the domain of a set of objects $O = (O_1, O_2, \ldots, O_n)$. The pair (O, d) is known as **metric space**. The similarity functions of the image descriptors are special cases of metric spaces.

Definition 4. A **Metric Access Method**(MAM) is a class of Access Method (AM) that is used to manage large volumes of metric data allowing insertions, deletions and searches [38].

2.3 Similarity Queries

In metric spaces it is possible to perform, among others, two kinds of similarity queries:

Definition 5. Given the query object O_q and the maximum search distance r_q, the **range query** $R_q(O_q, r_q)$ is used to retrieve all the objects in O that satisfy the following condition: $d(O_q, O_r) < r_q$.

Definition 6. Given the query object O_q and the value $k \in Z^+$, the **k-Nearest Neighbor Query** ($kNN(O_q, k)$) retrieve the k-closest objects in O that satisfy the following properties: $|O_r| = k$ and $d(O_q, O_r) \leq d(O_q, O_s) \forall O_s \in O$.

3 Related Work

The most common way to reduce the number of one-to-many comparisons during fingerprint retrieval is to partitionate the database using fingerprint classification techniques. They can be divided into two main categories: exclusive and continuous classification.

The former uses information related to the pattern of ridges and valleys that can be found in fingerprints to partitionate the fingerprint database into mutual exclusive bins. In this sense, once the fingerprint query image is classified, the image candidates are searched in the corresponding bin. Further, this kind of approach can be subdivided into four subcategories depending on the type of information used for exclusive classification, namely, ridge-, orientation field-, singularity-, and structural-based information. In continuous classification approaches, fingerprint images are represented by feature vectors. Similarities among fingerprint images are established by the distance in the feature space of their corresponding feature vectors. This approach is closely related to a fingerprint database indexing problem.

Ridge-based approaches use traditionally the information of the structure's frequency of the fingerprint ridges for classification purposes. The work proposed by Fitz et al. [5] uses the frequency spectrum of fingerprints, obtained by applying a hexagonal Fourier Transform, to classify fingerprints into three classes: whorl, loops, and arches. A wedge-ring detector is used to partitione the frequency domain images into non-overlapping areas where the pixel values were summed up to form a feature vector. Once the feature vector was found, it was compared to the reference feature vectors of each class and further classification is performed by using a nearest neighbor method.

To capture the structure of fingerprint ridges, some works develop mathematical models to characterize the fingerprint images [7, 6]. Chong et al. [6] use, for example, B-splines curves to approximate the shape of each of the fingerprint ridges. Then, similar orientation ridges are grouped together to obtain a global shape representation of fingerprints, which is used for classification.

Approaches based on orientation field use the local average orientations of fingerprint ridges to classify fingerprints. Halici et al. [8] use the block orientation fields of fingerprints and certainty measures to generate the fingerprint feature vectors. For the sake of feature dimensionality reduction, they used a SOM neuronal network. Moreover, a second layer was

added to the neuronal network's architecture to improve the overall classification accuracy.

Fingerprint singularities have been widely used for classification [9, 10]. They can be defined as the local regions where the fingerprint ridges present some physical properties. Karu et al. [10] extract the singularities that can be found in the fingerprints to classify them, considering the location and the number of detected singularities.

Structural approaches use topology information of fingerprints for classification purposes. Maio et al. [11] segment the orientational field of fingerprint images to represent the fingerprints as relational graphs. For each class of fingerprints, a model relational graph is created. An inexact graph matching algorithm is used to classify fingerprint images.

Although the search spaces can be reduced in exclusive classification approaches, there are some shortcomings that should be considered: (1) some fingerprints present properties of more than one class and therefore they cannot be assigned into just one bin, (2) natural distribution of fingerprints is not uniform and therefore, even performing binning in the original database, the number of one-to-many comparisons can still be high [1], and (3) some of the characteristics used for binning are not easy to detect due to the presence of noise, ambient conditions, etc.

On the other hand, Germain et al. [35] proposed a continuous system to index fingerprint databases using flash hashing. For that purposes, the location and orientation of minutiaes, as well as the number of ridges among them are used to generate feature vectors. Some information related to the feature vectors is obtained and used to create the image indices that are added to a multi map memory structure and used latter during fingerprint retrieval.

More recently, Tan et al. [34] compared two fingerprint identification approaches based on: (a) classification followed by verification, and (b) indexing followed by verification. Their classification approach uses Genetic Programming to generate compositor operators applied to some features extracted of the fingerprint orientation fields. A Bayesian classifier is them used to classify fingerprints. Their indexing approach is based on the work of Germain [35]. However, as a result of the retrieval process, a list of N fingerprint candidates is retrieved for the verification phase. The idea is to determine the correspondence degree between the query image and the database images. They concluded that the indexing-based approach outperforms the classification considering the size of the search spaces.

Although the search spaces are reduced in both approaches ([35, 34]), they are mainly based on some singularities that can be found in fingerprint images. Furthermore, the accurate detection of these singularities depend highly on the quality of fingerprint images. Moreover, their computation often involves high computational costs, that will affect directly the fingerprint recognition time. In addition, they both use flash hashing for indexing

[1] Cappelli et al. [27] proved that the distribution of fingerprint classes is not uniform (93.4% of fingerprints are among a set of three classes)

purposes and we believe that by using metric access methods the query processing time will be improved. Thus, we will consider more specifically textural information presented in fingerprints for feature extraction purposes, since they retain the discriminating power of fingerprints and Metric Access Methods (MAM) for their indexing. The description of the MAM used in our approach is beyond the scope of this paper, however a brief description is presented in section 7.

4 System Overview

The architecture of our system, shown in Figure 1, provides the necessary functionality for the fingerprint-image retrieval application. The system itself can be divided into two main subsystems, namely, the enrollment- and the query-subsystem. The enrollment-subsystem is responsible for acquiring the information that will be stored in the database for later use. On the other side, the query subsystem is responsible for retrieving similar fingerprints from the database according to the user's query image. Our system operates as follows:

1. Enrollment-subsystem: several fingerprint images are first captured (arrow labeled 1 in Figure 1) and then processed by a center point area detection module, which finds and marks a Region of Interest (ROI) within the fingerprint (module 1, arrow 2). The fingerprint ROI is represented by its central part, since most of the category information is contained in it. A region of 64 x 64 pixels is used for marking the ROI. The feature extraction module uses the feature extraction algorithms in the descriptor library (module B, arrow 3) for extracting the features (arrow 4) that are indexed by a metric access method for later use.

2. Query-subsystem: it receives as input a fingerprint query image from the user (arrow 1). The fingerprint ROI is then detected (module A, arrow 2) and the feature extraction module uses the feature extraction algorithms in the descriptor library to extract the feature vectors from the query image (module B with arrows 3 and 4, respectively). The query image feature vector is used to rank the database images according to their similarity to the query image (module C). For that purposes, a distance computation algorithm is selected from the descriptor library (arrow 5) and the metric access method is used to speed up the retrieval (arrow 6). Finally, the most similar database images are ranked (arrow 7) and returned to the user (arrow 8).

Subsequent sections will also describe the details of the system components.

5 Center Point Area Detection

In our approach, we have considered the core point as the center point for selecting a singular point area from which the feature vectors will be computed. The steps used for core detection are [14]:

1. Estimation and smoothing of the directional fields of the fingerprint input image.

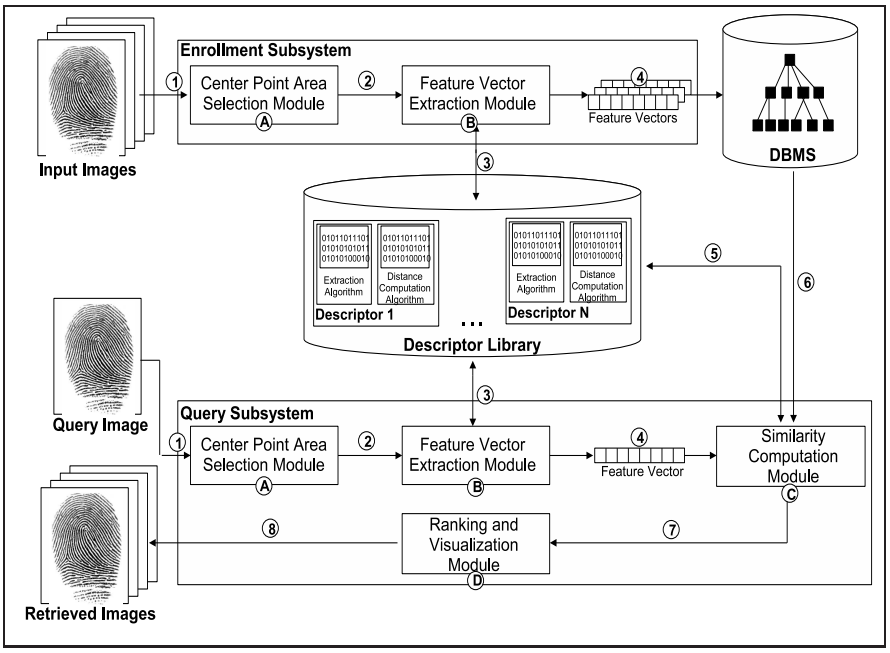

Figure 1: Architecture of the proposed system.

2. Computation of the Poincaré index, in each (8×8) block. This index is defined as follows:

$$\text{Poincare(i,j)} = \frac{1}{2\pi} \sum_{k=0}^{N-1} \Delta(k) \tag{1}$$

$$\Delta(k) = \begin{cases} \delta(k) & \text{if } |\delta(k)| < \frac{\pi}{2} \\ \pi + \delta(k) & \text{if} \delta(k) \leq -\frac{\pi}{2} \\ \pi - \delta(k) & \text{otherwise} \end{cases} \tag{2}$$

$$\delta(k) = \theta(X(k^{'}), Y(k^{'})) - \theta(X(k), Y(k)) \tag{3}$$

where $k^{'} = (k+1) \bmod (N)$ and $\theta(i,j)$ is the directional field of the fingerprint image. $X(k)$ and $Y(k)$ are the coordinates of the blocks that are in the closed curve with N blocks. If the Poincaré index has a value of $1/2$, then the current block is the core block. The center of this block is then the core point. If more than two cores are detected go back to step 1 using a larger smoothing parameter for the directional fields.

Once the center point is obtained, a center point area can be easily defined. An image of size 64 by 64 pixels around the core point is then cropped, as shown in Figure 2.

6 Feature Extraction

Wavelets have proved their efficiency in image retrieval problems due to their capability in capturing both texture and shape information [40, 41]. The Wavelet subband and multi-

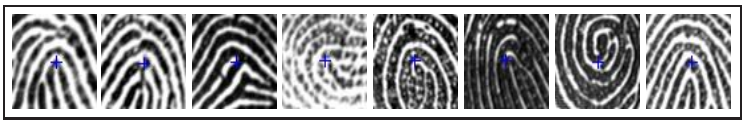

Figure 2: Some image samples of the center point area detected of 8 different fingerprints from FVC-2002 Database [31].

resolution decomposition are extremely adapted to compute relevant information about the structure of data, and thus it allows describing images, preserving their basic content [1]. In this section, we present the wavelet-based feature extraction approaches we have considered in our system.

6.1 Texture Feature Extraction

The texture found in images represents a powerful discriminating feature for both image classification and retrieval. Although there does not exist a formal definition of texture, it can be understood as the basic primitives in images, whose spatial distribution creates some visual patterns. Thus, the goal of a texture feature extraction method is to create a feature vector that captures the image texture information and preserves, at the same time, its content.

Considering that the ridges and valleys of fingerprints form a textural pattern, it is then possible to capture discriminatory information trough their textural representations. Further, the feature vectors are indexed and stored for image retrieval purposes.

6.2 Wavelet-based Feature Extraction

The use of the Wavelet transform for texture description is motivated by two reasons [40]: (1) it integrates both multiresolution and space-frequency properties naturally, and (2) has demonstrated good accuracy for texture analysis and classification [40].

6.2.1 Wavelet Transform Review

The Wavelet Transform decomposes a signal $f(x)$ with a family of functions that are obtained through dilations and translations of a kernel function $\psi(x)$, called the mother wavelet, which is localized in both spatial and frequency domains. This family of functions is denoted by:

$$\psi_{m,n}(x) = 2^{\frac{-m}{2}}\ \psi(2^m x - n) \tag{4}$$

where m, n $\in \mathbb{Z}^+$ indicate the dilations and translations, respectively. To construct the mother wavelet $\psi(x)$ a so-called scaling function $\phi(x)$ is needed:

$$\phi(x) = \sqrt{2} \sum_k h(k)\ \phi(2x - k) \tag{5}$$

Then, the wavelet kernel $\psi(x)$ is determined as follows:

$$\psi(x) = \sqrt{2} \sum_{k} g(k)\ \phi(2x - k) \tag{6}$$

where:

$$g(k) = (-1)^k\ h(1 - k) \tag{7}$$

The explicit forms of $\phi(x)$ and $\psi(x)$ are not required to perform the wavelet transform, because it only depends on the coefficients $h(k)$ and $g(k)$ with low- and high-pass characteristics, respectively. The L-level decomposition of the signal $f(x)$ can be written as:

$$\begin{aligned} f(x) &= \sum_{n} c_{0,n}\ \phi_{0,n}(x) \\ f(x) &= \sum_{n} c_{L,n}\ \phi_{L,n}(x) + \sum_{l=1}^{L+1} \sum_{n} d_{l,n}\ \phi_{l,n}(k) \end{aligned} \tag{8}$$

where the coefficients $c_{0,n}$ are given and the coefficients $c_{L,n}$ and $d_{l,n}$, both at scale l, are obtained by the coefficients $c_{l-1,n}$ at scale $l - 1$ trough:

$$\begin{aligned} c_{l,n} &= \sum_{k} c_{l-1,n}\ h(k - 2n) \\ d_{l,n} &= \sum_{k} c_{l-1,n}\ g(k - 2n) \end{aligned} \tag{9}$$

where $1 \leq l \leq L + 1$. A recursive wavelet decomposition can be obtained through $h(k)$ and $g(k)$ in Equation 9. The same process can be viewed as the convolution of signal $c_{l-1,n}$ with the impulse responses $\overline{h(n)} = h(-n)$ and $\overline{g(n)} = g(-n)$ of the low- and high-pass filters H and G, respectively (also known as quadrature filters), and then by downsampling the filtered signals by a factor of 2. The 2-D wavelet and scaling functions can be expressed as the tensor products of their 1-D complements:

$$\begin{aligned} \phi_{LL}(x, y) &= \phi(x)\phi(y) \qquad \psi_{LH}(x, y) = \phi(x)\psi(y) \\ \psi_{HL}(x, y) &= \psi(x)\phi(y) \qquad \psi_{HH}(x, y) = \psi(x)\psi(y) \end{aligned} \tag{10}$$

where $\phi_{LL}, \psi_{LH}, \psi_{HL}$ and ψ_{HH} represent the Low-Low, Low-High, High-Low, and High-High subbands, respectively.

6.2.2 The Tree-Structured Wavelet Transform

The Tree-Structured Wavelet Transform decomposes recursively the output of each of the subbands. This kind of decomposition is based on the fact that for some kinds of texture the most relevant information exist in the middle subbands. To avoid a full recursive decomposition, Chang et al. [24] proposed an energy-based criterion to decide which image should be further decomposed. If the energy in a subband is very similar to the maximum energy

of a subband at the same level, the further decomposition is not applied. However, for the sake of image retrieval, a fixed tree decomposition is convenient, since it facilitates distance computations and hence data browsing. Considering that the subband HH often leads to unstable features, recursively decomposition is done only in the LL, LH, HL subbands.

6.2.3 Gabor Wavelets

A general 2-D Gabor function $\psi(x, y)$ is defined as:

$$\psi(x,y) = \left(\frac{1}{2\pi\sigma_x\sigma_y}\right) exp\left[-\frac{1}{2}\left(\frac{x^2}{\sigma_x^2}+\frac{y^2}{\sigma_y^2}\right)+2\pi jWx\right] \tag{11}$$

where the spatial coordinates (x, y) denote the centroid localization of the elliptical Gaussian window. The parameters σ_x and σ_y are the space constants of the Gaussian envelop along the x- and y-axes, respectively. The Fourier transform $G(u, v)$ of the Gabor function $\psi(x, y)$ can be written as:

$$G(u,v) = exp\left[\frac{-1}{2}\left(\frac{(u-W)^2}{\sigma_u^2}+\frac{v^2}{\sigma_v^2}\right)\right] \tag{12}$$

where W represents the frequency of the sinusoidal plane along the horizontal axis and the frequency components in x- and y-direction are denoted by the pair (u, v), while $\sigma_u = 1/2\pi\sigma_x$ and $\sigma_v = 1/2\pi\sigma_y$. Considering the non-orthogonal basis set formed by the Gabor functions, a localized frequency description can be obtained by expanding a signal with this basis.

Self-similar class functions, known as Gabor Wavelets, can be generated by dilations and rotations of the mother wavelet $\psi(x, y)$, i.e.:

$$\psi_{m,n}(x,y) = a^m\psi_{x',y'}, \quad a>1 \tag{13}$$

considering $m = 1, \ldots S$ and $n = 1, \ldots K$. S and K denote the total number of dilations and orientations, respectively, and:

$$\begin{bmatrix} x' \\ y' \end{bmatrix} = a^{-m}\begin{bmatrix} cos\theta_n & sin\theta_n \\ -sin\theta_n & cos\theta_n \end{bmatrix}\begin{bmatrix} x \\ y \end{bmatrix} \tag{14}$$

where $\theta = n\pi/K$ and θ is the rotation angle. To ensure that the energy is independent of m, a scale factor a^{-m} is introduced. Considering the redundant information presented in the filtered images due to the non-orthogonality of the Gabor Wavelets, Manjunath et al. [19] designed a strategy to reduce the redundancy of the Gabor Wavelets Filterbank, where the half-peak magnitude of the filter responses touch each other in the frequency spectrum:

$$a = \left(\frac{U_h}{U_l}\right)^{\frac{1}{S-1}} \qquad \sigma_u = \frac{(a-1)U_h}{(a+1)\sqrt{2ln2}} \tag{15}$$

$$\sigma_v = tan\left(\frac{\pi}{2K}\right)\left[U_h - 2ln2\left(\frac{\sigma_u^2}{U_h}\right)\right]\left[2ln2 - \frac{(2ln2)^2\sigma_u^2}{U_h^2}\right]^{-\frac{1}{2}} \tag{16}$$

where $W = U_h$. The parameters U_h and U_l are used, respectively, to denote the upper and lower center frequencies of interest.

6.2.4 Feature Representation

Considering the spatial homogeneity present in fingerprint images, the mean (μ_{mn}) and the standard deviation (σ_{mn}) of the energy distribution are used to form the feature vector $\overline{f}$:

$$\mu_{mn} = \frac{1}{MN} \iint |W_{mn}(x,y)|\, dxdy \tag{17}$$

$$\sigma_{mn} = \sqrt{\iint \left(W_{mn}(x,y) - \mu_{mn}\right)^2 dxdy} \tag{18}$$

For the Tree-Structured Wavelet Transform the values of $|W_{mn}(x,y)|$ correspond to the energy distribution in one of the three subbands: LL, LH, and HL. Thus, the subindices m and n are integers that stand for the decomposition level and the current subband ($m = 1, 2, \ldots, L$ and $n = 1, 2, 3$), respectively. The feature vector $\vec{f}$ is formed as follows:

$$\vec{f}_{TSWT} = [\mu_{11}, \sigma_{11}, \mu_{12}, \sigma_{12}, \mu_{13}, \sigma_{13}; \ldots; \mu_{L1}, \sigma_{L1}, \mu_{L2}, \sigma_{L2}, \mu_{L3}, \sigma_{L3}] \tag{19}$$

In the case of the Gabor Wavelet Transform, the values of $|W_{mn}(x,y)|$ denote the energy distribution of the transform coefficients after convolving an image I with the Gabor Wavelet $\psi_{m,n}$. Considering a total number of $S = 6$ scales and $K = 16$ orientations, the resulting feature vector is computed as follows:

$$\vec{f}_{GW} = [\mu_{11}, \sigma_{11}; \mu_{12}, \sigma_{12}; \ldots \mu_{616}, \sigma_{616}] \tag{20}$$

7 Feature Indexing

In this section, we present the different similarity measures studied in our work and the Metric Access Method used for feature indexing.

7.1 Similarity Measures

A key component of a CBIR system are the similarity measure functions used for computing the similarity among images. This affirmation is valid because the retrieval performance depends not only on the effectiveness of the image features, but also on how good the similarity measures are. Thus, different similarity measures should be explored in order to improve the retrieval effectiveness. Let $\vec{x} = (x_1, x_2, \ldots, x_n)$ and $\vec{y} = (y_1, y_2, \ldots, y_n)$ be two feature vectors of dimension n, Table 1 presents the similarity measures studied in our work.

7.2 Metric Access Method

To speed-up the retrieval we have used a dynamic MAM known as Slim-tree [38]. The use of the Slim-tree in the fingerprint domain is attractive, since: (1) fringerprints can be inserted and deleted even after its creation, due to their dynamicity, (2) similarity queries such kNN and range queries are supported and therefore CBIR applications are possible,

Evaluated Similarity Measures	
Measure	Equation
Bray Curtis	$d_{BC} = \sum_{i=1}^{n} \frac{\lvert x_i - y_i \rvert}{x_i + y_i}$
Canberra	$d_C = \sum_{i=1}^{n} \frac{\lvert x_i - y_i \rvert}{\lvert x_i \rvert + \lvert y_i \rvert}$
Euclidean	$d_E = \sqrt{\sum_{i=1}^{n} (x_i - y_i)^2}$
Manhattan	$d_M = \sqrt{\sum_{i=1}^{n} \lvert x_i - y_i \rvert}$
Squared Chord	$d_{SC} = \sum_{i=1}^{n} (\sqrt{x_i} - \sqrt{y_i})^2$
Square Chi-Squared	$d_{SChi} = \sum_{i=1}^{n} \frac{(x_i - y_i)^2}{x_i + y_i}$

Table 1: Evaluated Similarity Measures

(3) overlapping between nodes is minimized and thus the retrieval speed is increased and (4) it can handle large amount of data in an efficient manner even after growing the database size due to the scalability property. Furthermore, the Slim-tree has outperformed the well known M-tree indexing structure [36].

8 Experiments

In this section we present the experimental setup we conducted in our study, as well as the effectiveness of the discussed feature extraction methods using the precision versus recall curves.

8.1 Databases

We used for our experiments the Bologna FVC-2002 database [31]. The use of these database was attractive because of its peculiarities. It consists in four different databases (DB1, DB2, DB3, and DB4) collected by different sensors/technologies. Each database contains 8 impressions per fingerdeep (**d**) and is 110 fingers wide (**w**). The size of each fingerprint image, as well as its resolution, vary in these collections. In the case of the DB1, fingerprints are of size 388x374 pixels with a resolution of 500 dpi. For the DB2, images are 296x560 pixels and have a resolution of 569 dpi. In the DB3, each fingerprint image has 300x300 pixels and a resolution of 500 dpi. The DB4 was created using a software for generating synthetic fingerprints [42, 43]. In this case, images have a size of 288x384 pixels and about 500 dpi. These datasets are challenging since there are some variations within

fingerprints of the same individuals finger. These variations include: rotations, translations, and the presence of low quality in images.

8.2 Effectiveness Evaluation

The retrieval effectiveness of our system was measured in terms of precision and recall [15], since they have been widely used to evaluate retrieval effectiveness. Precision is defined as the fraction of the retrieved images that are relevant to the given query, while the recall represents the proportion of relevant images among the retrieved ones. Thus, retrieved images are considered as a match if they belong to the same class of the query image. Considering the query image q, and the number of correct, missed, and false candidates (n_c, n_m, and n_f, respectively), the precision p_q in the first R retrieved images is defined as follows:

$$p_q = \frac{n_c}{n_c + n_f} = \frac{n_c}{R} \tag{21}$$

The recall r_q of the such similar candidates S of the query image q is defined as:

$$r_q = \frac{n_c}{n_c + n_m} = \frac{n_c}{S} \tag{22}$$

8.3 Experiments

Our system was tested independently in each of the four databases and each of the database images was considered as a query image. Thus, a total number of 880 fingerprint queries were performed per database. The experiments were carried out by using a total number of 36 different image descriptors. To generate them we have combined six different wavelet-based feature extraction functions with the six similarity measures presented in subsection 7.1. The six different types of Wavelets include: Gabor Wavelets, TSWT using Haar, Daub 4-Tap, Daub 8-Tap, Daub 16-Tap, and Spline Wavelets.

The first group of experiments were conducted to determine which combination of wavelet-based feature extraction algorithms with similarity measures presents the highest retrieval effectiveness in each of the four databases. Thus, six different figures were generated (Figures 3, 4, 5, 6, 7, and 8). Each of them present the averaged recall achieved per fingerprint extraction algorithm with each of the six different similarity measures.

From Figure 3 we can observe that for each of the four databases, the highest retrieval effectiveness for the the Gabor Wavelets was obtained by using the Square Chord similarity measure. The fact that the distance in each dimension is first obtained by performing the square root and then by applying the power of two, before summation, reduces the emphasis on those features with large dissimilarity.

Observing Figure 4, one can conclude that the best similarity measures for the TSWT using Spline Wavelets are the Manhattan and the Euclidean distances. That is because both

of them measure the absolute differences in each feature dimension in order to increase the retrieval effectiveness. However, one benefit of the Manhattan distance is that it requires less computational operations than the Euclidean distance.

For the case of the TSWT using Haar Wavelets the best retrieval indices were obtained by using the Mahattan distance, as seen in Figure 5. In the case of the TSWT using Daubechies 4-Tap, 8-Tap, and 16-Tap the best retrieval effectiveness was achieved by using the Square Chi-Squared similarity measure, as shown in Figures 6, -7, and 8.

The main objective of the fingerprint identification approach proposted in this paper is to ensure that the relevant image databases are retrieved, and not to determine whether fingerprint images are the same. Therefore, our system is suitable for both fingerprint image indexing and retrieval. Note also that the databases used in these experiments do not have been acquired in real environments [31], being, therefore, useful for testing our system in extreme conditions. In fact, we do believe that the retrieval accuracy can be increased if we consider real world fingerprint collections.

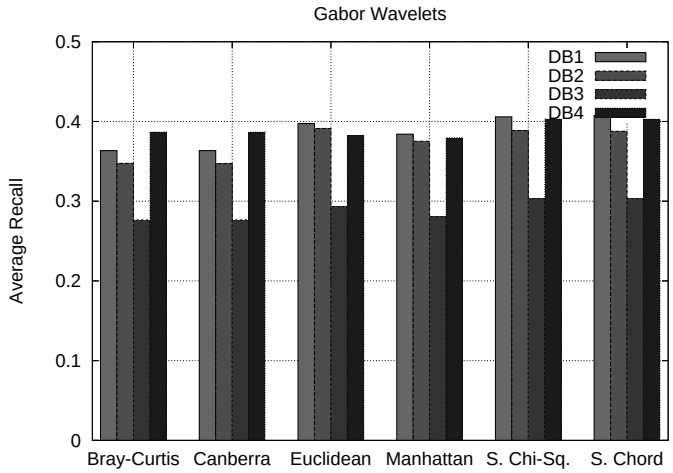

Figure 3: Average Recall using Gabor Wavelets.

The goal of the second group of experiments is to determine the best pair of feature extraction algorithms and similarity measures. Thus, for each of the four databases we have considered the average retrieval effectiveness of all 36 image descriptors. The best combinations are then found and for each of the 4 databases, we found the best wavelet feature extraction algorithms with their respective similarity measures. Considering the Figures 9, 10, 11, and 12 it is clear that Gabor Wavelets outperformed the other approaches in terms of retrieval accuracy. This is due to the fact that the Gabor Wavelets capture much useful information at different orientations if compared with the traditional Tree-Structured Wavelet Transforms, which does not take into account this specific information. Thus, a

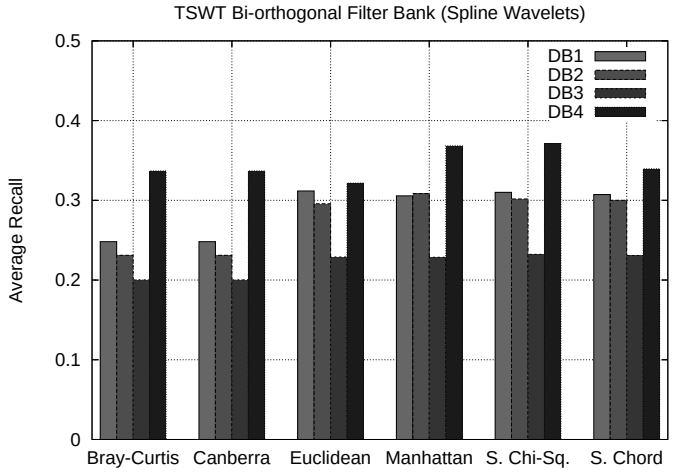

Figure 4: Average Recall using a TSWT Bi-orthogonal Filter Bank (Spline Wavelets).

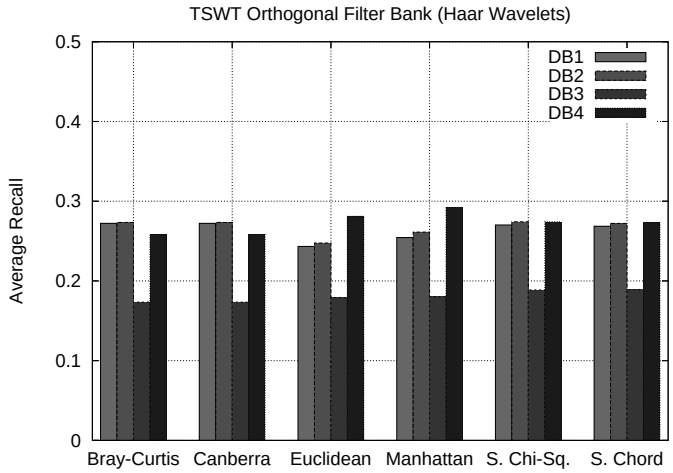

Figure 5: Average Recall using a TSWT Orthogonal Filter Bank (Haar Wavelets).

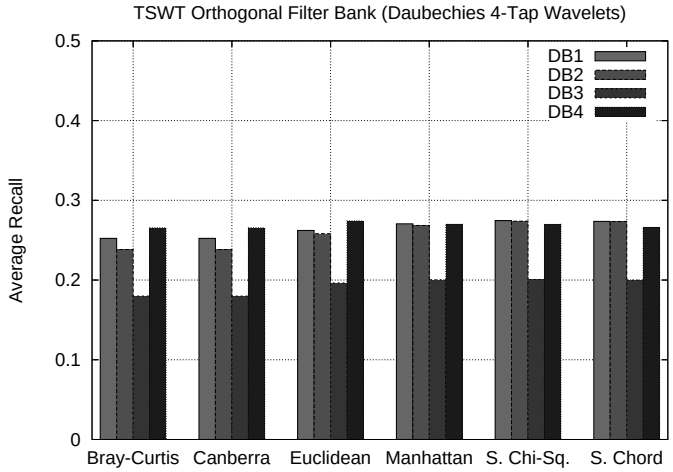

Figure 6: Average Recall using a TSWT Orthogonal Filter Bank (Daubechies 4-Tap).

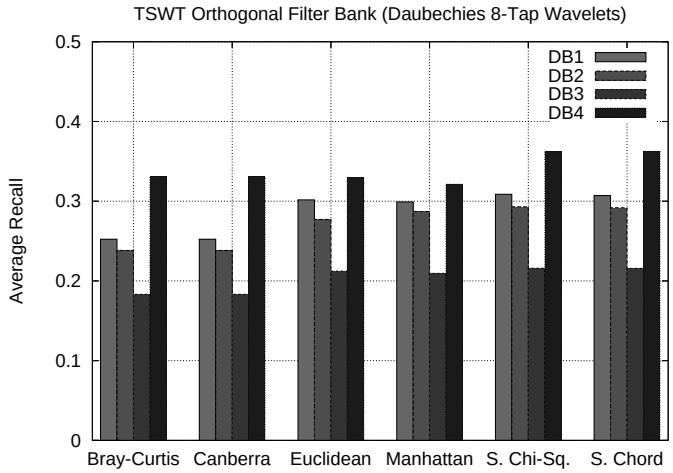

Figure 7: Average Recall using a TSWT Orthogonal Filter Bank (Daubechies 8-Tap).

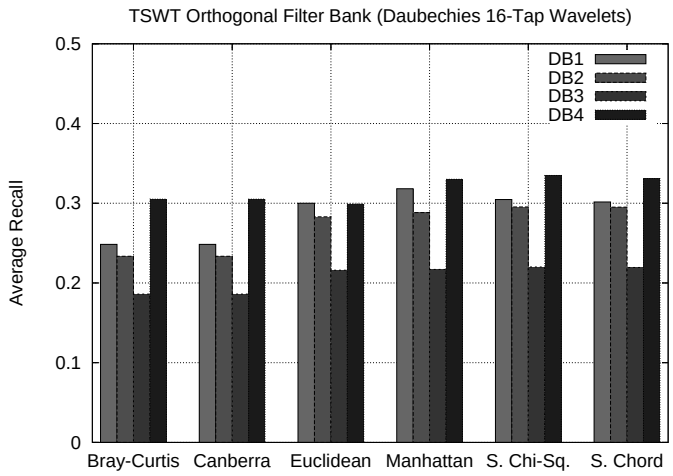

Figure 8: Average Recall using a TSWT Orthogonal Filter Bank (Daubechies 16-Tap).

more precise retrieval was performed due to the Gabor Wavelets flexibility in controlling the orientation information.

9 Conclusions

This paper has investigated the possibility of applying texture-based image retrieval techniques to reduce the search space for fingerprint identification. More specifically, we have proposed a novel approach to characterize fingerprint images by using different types of Wavelet transforms and similarity measures.

The retrieval effectiveness of the different image descriptors was compared by analyzing the results in terms of precision and recall. For all experiments, the best result was achieved by the Gabor Wavelet Transform combined with the Square Chord similarity measure. This fact relies basically on its flexibility to model the orientation and the scale information in images. Moreover, depending on the desired accuracy the descriptor parameter values can be adapted. The lack of this flexibility has influenced the retrieval performance of the Tree-Structured Wavelet Transform (TSWT), since it is not able to capture relevant information in different orientations.

It is important to notice that the databases used in our experiments do not reflect real acquisition conditions in the sense that image present abnormal distortions, including noise, significant rotations, and translations [31]. In this context, future work includes the use of databases containing more realistic fingerprint images. In this case, we expect that the retrieval effectiveness of our image descriptors will be considerably improved. In addition,

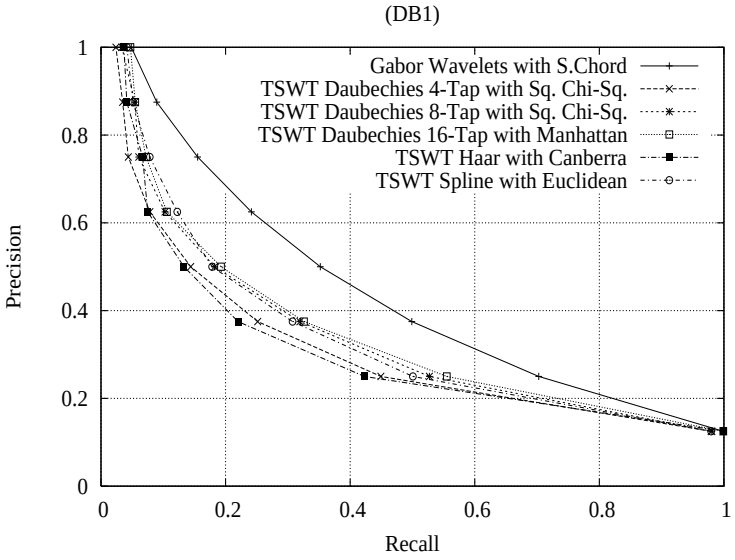

Figure 9: Averaged Precision vs. Recall curves of the best image descriptors for the DB1.

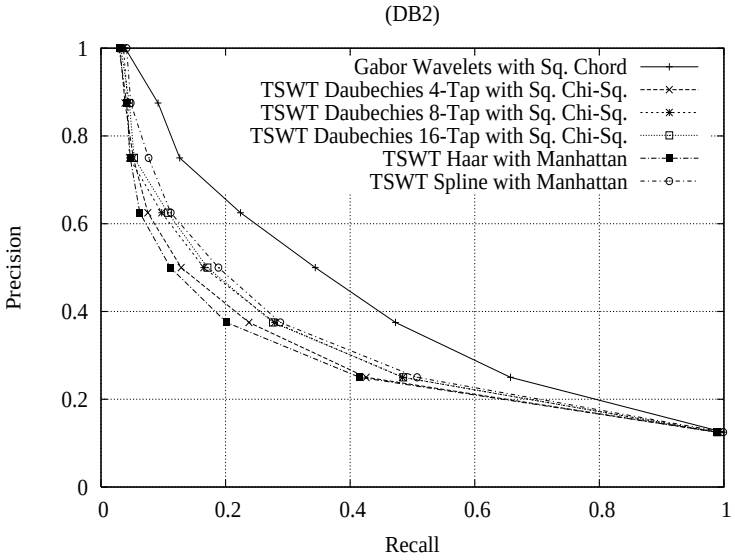

Figure 10: Averaged Precision vs. Recall curves of the best image descriptors for the DB2.

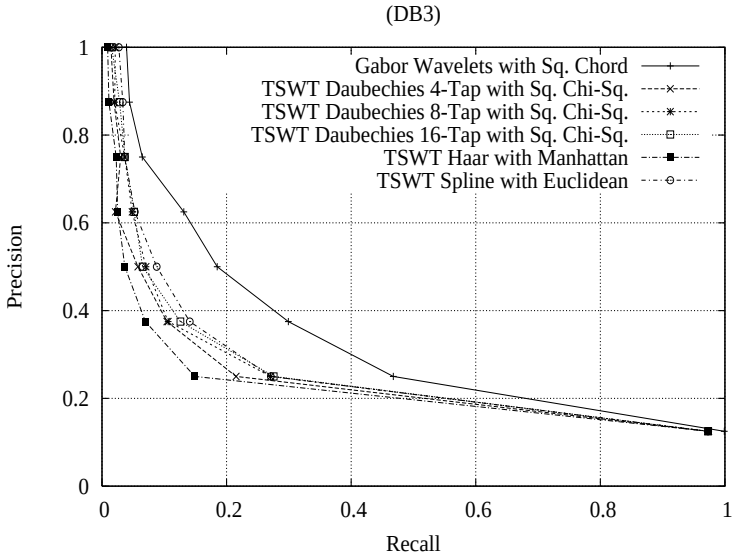

Figure 11: Averaged Precision vs. Recall curves of the best image descriptors for the DB3.

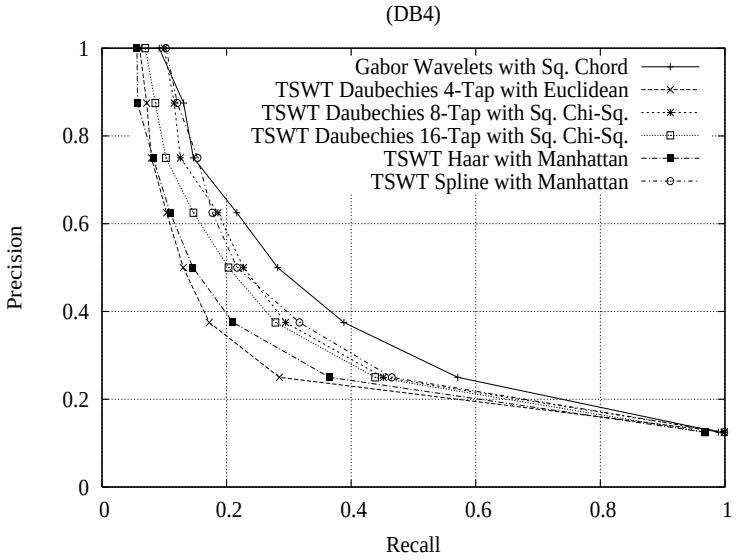

Figure 12: Averaged Precision vs. Recall curves of the best image descriptors for the DB4.

we also plan to study the impact of using different metric access methods for fingerprint identification.

References

[1] Charles K. Chui, *An introduction to wavelets*, Academic Press Professional Inc.(1992), San Diego, CA, USA, isbn. 0-12-174584-8.

[2] Wei Zhao and Rama Chellappa and P. Jonathon Phillips and Azriel Rosenfeld, *Face recognition: A literature survey*, ACM Computing Surveys, **35** (4), 399–458 (December 2003).

[3] Richard P. Wildes, *Iris Recognition: An Emerging Biometric Technology*, Proceedings of the IEEE, **85** (9), 1348–1363 (September 1997).

[4] Vishvjit S. Nalwa, *Automatic On-Line Signature Verification*, Proceedings of the IEEE, **85** (2), 215–239 (February 1997).

[5] Fitz and Green, *Fingerprint classification using a hexagonal fast Fourier Transform*, Pattern Recognition, **29** (10), 1587–1597 (1996).

[6] Chong and Ngee and Jun and Gay, *Geometric Framework for fingerprint image classification*, Pattern Recognition, **30** (9), 1475–1488 (1997).

[7] Anil K. Jain and Silviu Minut, *Hierarchical Kernel Fitting for Fingerprint Classification and Alignment*, 16th International Conference on Pattern Recognition 2002, **2**, 469–473 (2002).

[8] Halici and Ongun, *Fingerprint classification through self-organizing feature maps modified to treat uncertainties*, Proceedings of the IEEE, **84** (10), 1497–1512 (1996).

[9] Lin Hong and Anil K. Jain, *Classification of Fingerprint Images*, Proceedings of the IEEE, 11th Scandinavian Conference on Image Analysis, June 7-11, Kangerlussuaq, Greenland, (1999).

[10] Kalle Karu and Anil K. Jain, *Fingerprint Classification*, Pattern Recognition, **29** (3), 223–231 (1999).

[11] D. Maio and D. Maltoni, *A Structural Approach to Fingerprint Classification*, ICPR '96: Proceedings of the International Conference on Pattern Recognition (ICPR '96) Volume III-Volume 7276, 578–585 (1996).

[12] Anders Eriksson and Par Wretling, *How flexible is the human voice? - A case study of mimicry*, Proceedings of EUROSPEECH, **2**, 1043–1046 (1997).

[13] Mark S. Nixon and John N. Carter, *Advances in automatic gait recognition*, Sixth IEEE International Conference on Automatic Face and Gesture Recognition, **85** (2), 139–144 (May 2004).

[14] Anil K. Jain and Salil Prabhakar and Lin Hong, *A Multichannel Approach to Fingerprint Classification*, IEEE Transactions on Pattern Analysis and Machine Intelligence, **21** (4), 348–359 (1999).

[15] William I. Grosky and Ramesh Jain and Rajiv Mehrotra, *Handbook of Multimedia Information Management*, Prentice-Hall.(1997), isbn. 0-13-207325-0.

[16] A. Califano and R. Mohan, *Multidimensional Indexing for Recognizing Visual Shapes*, IEEE Transactions on Pattern Analysis and Machine Intelligence, **16** (4), 373–392 (1994).

[17] R. W. Picard and T. P. Minka, *Vision texture for annotation*, Multimedia Systems, **3** (1), 3–14 (1995).

[18] Michael J. Swain and Dana H. Ballard, *Color indexing*, International Journal of Computer Vision, **7** (1), 11–32 (1991).

[19] Bangalore S. Manjunath and Wei-Ying Ma, *Texture Features for Browsing and Retrieval of Image Data*, IEEE Transactions on Pattern Analysis and Machine Intelligence, **18** (8), 837–842 (1996).

[20] Ingrid Daubechies, *The wavelet transform, time-frequency localization and signal analysis*, IEEE Transactions on Information Theory, **36** (5), 961–1005 (1990).

[21] Stephane G. Mallat, *A theory for multiresolution signal decomposition: the wavelet representation*, IEEE Transactions on Pattern Analysis and Machine Intelligence, **11** (7), 674–693 (1989).

[22] Michael Unser, Akram Aldroubi and Murray Eden, *A family of polynomial spline wavelet transforms*, Signal Processing, **30** (2), 141–162 (1993).

[23] Tai Sing Lee, *Image Representation Using 2D Gabor Wavelets*, IEEE Transactions on Pattern Analysis and Machine Intelligence, **18** (10), 959–971 (1996).

[24] Tianhorng Chang and C.-C. Jay Kuo, *Texture analysis and classification with tree-structured wavelet transform*, IEEE Transactions on Image Processing, **2** (4), 429–441 (1993).

[25] Eero P. Simoncelli and William T. Freeman, *The Steerable Pyramid: A Flexible Architecture for Multi-Scale Derivative Computation*, International Conference on Image Processing, **3**, 444–447 (1995).

[26] Sharath Pankanti and Salil Prabhakar and Anil K. Jain, *On the individuality of fingerprints*, IEEE Transactions on Pattern Analysis and Machine Intelligence, **24**(8), 1010–1025 (2002).

[27] Raffaele Cappelli and Dario Maio and Davide Maltoni and Loris Nanni, *A two-stage fingerprint classification system*, WBMA '03: Proceedings of the 2003 ACM SIGMM workshop on Biometrics methods and applications, 95–99 (2003).

[28] Anil K. Jain, Lin Hong, Sharath Pankanti and Ruud Bolle, *An identity-authentication system using fingerprints*, Proceedings of the IEEE, **85**(9), 1365–1388 (1997).

[29] Anil K. Jain and Lin Hong and Ruud M. Bolle, *On-Line Fingerprint Verification*, IEEE Transactions on Pattern Analysis and Machine Intelligence, **19**(4), 302–314 (1997).

[30] Alessandra Lumini and Dario Maio and Davide Maltoni, *Continuous versus exclusive classification for fingerprint retrieval*, Pattern Recognition Letters, **18**(10), 1027–1034 (1997).

[31] Dario Maio and Davide Maltoni and Raffaele Cappelli and J. L. Wayman and Anil K. Jain, *FVC 2002: Second Fingerprint Verification Competition*, Proceedings of the 16th International Conference on Pattern Recognition 2002, **3**, 811–814 (2002).

[32] Nalini K. Ratha and Kalle Karu and Shaoyun Chen and Anil K. Jain, *A Real-Time Matching System for Large Fingerprint Databases*, IEEE Transactions on Pattern Analysis and Machine Intelligence, **18**(8), 799–813 (1996).

[33] Amit Mhatre and Srinivasa Palla and Sharat Chikkerur and Venu Govindaraju, *Efficient Search and Retrieval in Biometric Databases*, SPIE Defence and Security Symposium, **5779**, 265–273 (2005).

[34] Xuejun Tan and Bir Bhanu and YingQiang Li, *Fingerprint identification: classification vs. indexing*, Proceedings of the IEEE Conference on Advanced Video and Signal Based Surveillance, 151–156 (2003).

[35] Robert S. Germain and Andrea Califano and Scott Colville, *Fingerprint matching using transformation parameter clustering*, IEEE Computational Science and Engineering, **4**(4), 42–49 (1997).

[36] Paolo Ciaccia, Marco Patella and Pavel Zezula, *M-tree: An efficient access method for similarity search in metric spaces*, 23rd International Conference on Very Large Data Bases (VLDB'97), 426–435 (1997).

[37] Simone Santini and Ramesh Jain, *Similarity Measures*, IEEE Transactions on Pattern Analysis and Machine Intelligence, **21**(9), 871–883 (1999).

[38] Caetano Traina Jr. and Agma Traina and Christos Faloutsos and Bernhard Seeger, *Fast indexing and visualization of metric data sets using slim-trees*, IEEE Transactions on Knowledge and Data Engineering (TKDE), **14**(2), 244–260 (2002).

[39] Manesh Kokare and B. N. Chatterji and P. K. Biswas, *Comparison of similarity metrics for texture image retrieval*, Conference on Convergent Technologies for Asia-Pacific Region, TENCON '03, **2**, 571–575 (2003).

[40] Kai-Chieh Liang and Kuo, C.-C.J., *WaveGuide: a joint wavelet-based image representation and description system*, IEEE Transactions on Image Processing, **8**(11), 619–1629 (1999).

[41] Apostol Natsev and Rajeev Rastogi and Kyuseok Shim, *WALRUS: A Similarity Retrieval Algorithm for Image Databases*, IEEE Transactions on Knowledge and Data Engineering, **16**(3), 301–316 (May 2004).

[42] R. Cappelli and D. Maio and D. Maltoni and A. Erol, *Synthetic Fingerprint-Image Generation*. International Conference on Pattern Recognition, **3**, 471–474 (2000).

[43] R. Cappelli and D. Maio and D. Maltoni, *Synthetic Fingerprint-Database Generation*. International Conference on Pattern Recognition, **3**, 744–747 (2002).